Reversible multiple time scale molecular dynamics

M. Tuckerman, B. J. Berne, and G. J. Martyna

Citation: J. Chem. Phys. **97**, 1990 (1992); doi: 10.1063/1.463137
View online: http://dx.doi.org/10.1063/1.463137
View Table of Contents: http://jcp.aip.org/resource/1/JCPSA6/v97/i3
Published by the American Institute of Physics.

Reversible multiple time scale molecular dynamics

M. Tuckerman[a] and B. J. Berne
Department of Chemistry, Columbia University, New York, New York 10027

G. J. Martyna
Department of Chemistry, University of Pennsylvania, Philadelphia, Pennsylvania 19104-6323

(Received 13 January 1992; accepted 17 March 1992)

The Trotter factorization of the Liouville propagator is used to generate new reversible molecular dynamics integrators. This strategy is applied to derive reversible reference system propagator algorithms (RESPA) that greatly accelerate simulations of systems with a separation of time scales or with long range forces. The new algorithms have all of the advantages of previous RESPA integrators but are reversible, and more stable than those methods. These methods are applied to a set of paradigmatic systems and are shown to be superior to earlier methods. It is shown how the new RESPA methods are related to predictor–corrector integrators. Finally, we show how these methods can be used to accelerate the integration of the equations of motion of systems with Nosé thermostats.

I. INTRODUCTION

Recently we have devised reference system algorithms for treating problems with separation in time scales (stiff oscillators in soft fluids,[1] disparate masses[2]) and/or forces that can be separated into short and long range components[3]). These algorithms run at much faster speeds than do the standard algorithms; sometimes with speedup factors on the order of 20 to 30. Some of these reference system methods are not reversible in time, and thus may exhibit numerical instabilities after very long times. Moreover, they can not be used in conjunction with hybrid Monte Carlo methods because these require strictly reversible molecular dynamics in order to satisfy detailed balance.[4]

In this paper we show how to make these reference system algorithms reversible in time. The starting point is the Trotter expansion of the classical Liouville propagator[5–7] and the reversable Trotter expansion.[11] From this we derive several new integrators for solving Newton's equations of motion. These new integration schemes involve the same number of force evaluations as the methods previously introduced, and therefore require no more CPU time in their execution. Furthermore, we find that making these methods reversible in time increases their stability over the RESPA and NAPA methods previously introduced.

In Sec. II we present a necessary review of the Liouville operator formalism. Trotter factorizations of the classical propagator can be used to derive simple integrators. In Sec. II A the velocity Verlet integrator as well as a new integrator, the *position* Verlet integrator is derived. In Sec. II C generalized Trotter factorizations are introduced. In Sec. III we treat the long range force problem and apply it to a particular example. In Sec. IV we treat the multiple time scale problem and apply it to the disparate mass mixtures in Sec. IV A and to systems with stiff oscillators in soft baths in Sec. IV B. In Sec. V we show how to combine these methods to treat problems with separation of time scales and long and short range forces. In Sec. VI we relate the Trotter expansion method to the more conventional predictor–corrector[8] methods. These methods are then extended in Sec. VII to treat constant temperature molecular dynamics simulations based on a Nosé heat bath.

[a] In partial fulfillment of the Ph.D. in the Department of Physics, Columbia University.

II. THE TROTTER EXPANSION OF THE LIOUVILLE PROPAGATOR

The Liouville operator L for a system of f degrees of freedom is defined in Cartesian coordinates as

$$iL = \{\cdots,H\} = \sum_{j=1}^{f}\left[\dot{x}_j\frac{\partial}{\partial x_j} + F_j\frac{\partial}{p_j}\right], \tag{2.1}$$

where $\Gamma = \{x_j,p_j\}$ are the position and conjugate momenta of the system, F_j is the force on the jth degree of freedom, and $\{\cdots,\cdots\}$ is the Poisson bracket of the system. L is a linear Hermitian operator on the space of square integrable functions of Γ. The classical propagator is then

$$U(t) = e^{iLt} \tag{2.2}$$

and the state of the system at time t is given by

$$\Gamma(t) = U(t)\Gamma(0), \tag{2.3}$$

and $U(t)$ is a unitary operator; i.e., $U(-t) = U^{-1}(t)$. In the following we will decompose the Liouville operator L into two parts such that

$$iL = iL_1 + iL_2. \tag{2.4}$$

For this decomposition the Trotter theorem[9] yields

$$\begin{aligned} e^{i(L_1+L_2)t} &= \left[e^{i(L_1+L_2)t/P}\right]^P \\ &= \left[e^{iL_1(\Delta t/2)}e^{iL_2\Delta t}e^{iL_1(\Delta t/2)}\right]^P \\ &\quad + O(t^3/P^2), \end{aligned} \tag{2.5}$$

where $\Delta t = t/P$. From this we define the discrete time propagator as

$$\begin{aligned} G(\Delta t) &= U_1\left(\frac{\Delta t}{2}\right)U_2(\Delta t)U_1\left(\frac{\Delta t}{2}\right) \\ &= e^{iL_1(\Delta t/2)}e^{iL_2\Delta t}e^{iL_1(\Delta t/2)}. \end{aligned} \tag{2.6}$$

 0021-9606/92/151990-12$06.00

Because the three factors in $G(\Delta t)$ are separately unitary it is easy to show that $G(t)$ is unitary, and therefore that $G^{-1}(t) = G^{\dagger}(t) = G(-t)$. This means that any integrator based on this Trotter factorization will be reversible.

The formal solution for any decomposition of the Liouvillian can be generated as follows: Let us define

$$\Gamma_1[\Delta t;\Gamma(0)] = U_1(\Delta t)\Gamma(0) \tag{2.7}$$

and

$$\Gamma_2[\Delta t;\Gamma(0)] = U_2(\Delta t)\Gamma(0) \tag{2.8}$$

to be, respectively, the state at time Δt when the system is propagated by $U_1(\Delta t)$ or $U_2(\Delta t)$ starting from the state $\Gamma(0)$. Then by applying the operators in Eq. (2.6) serially to $\Gamma(0)$ gives

$$\Gamma(\Delta t) = U_1\left(\frac{\Delta t}{2}\right) U_2(\Delta t) U_1\left(\frac{\Delta t}{2}\right)\Gamma(0)$$

$$= U_1\left(\frac{\Delta t}{2}\right) U_2(\Delta t)\Gamma_1\left[\frac{\Delta t}{2};\Gamma(0)\right], \tag{2.9}$$

$$\Gamma(\Delta t) = U_1\left(\frac{\Delta t}{2}\right)\Gamma_2\left\{\Delta t;\Gamma_1\left[\frac{\Delta t}{2};\Gamma(0)\right]\right\}, \tag{2.10}$$

$$\Gamma(\Delta t) = \Gamma_1\left(\frac{\Delta t}{2};\Gamma_2\left\{\Delta t;\Gamma_1\left[\frac{\Delta t}{2};\Gamma(0)\right]\right\}\right). \tag{2.11}$$

To generate this solution on a computer:

(a) Start with the initial state $\Gamma(0)$ and generate the motion under the propagator $e^{iL_1\Delta t/2}$. This gives the state $\Gamma_1[\Delta t/2;\Gamma(0)]$.

(b) Use the state just generated as the initial state and generate the motion using the propagator $e^{iL_2\Delta t}$. This gives the state $\Gamma_2\{\Delta t;\Gamma_1[\Delta t/2;\Gamma(0)]\}$.

(c) Start with state generated in (b) as the initial condition and generate the motion using $e^{iL_1\Delta t/2}$. This gives the final state $\Gamma(\Delta t)$ specified in Eq. (2.11).

The solution for a more complicated breakup proceeds analogously.

We note in passing that the Trotter expansion carried out to higher orders will yield higher order integrators. For example, to obtain an integrator good to $O(\Delta t^4)$ one would start with the Trotter expansion

$$e^{i(L_1+L_2)\Delta t} \approx e^{iL_1(\Delta t/2)} e^{iL_2(\Delta t/2)} e^{-iC(\Delta t^3/24)} \times e^{iL_2(\Delta t/2)} e^{iL_1(\Delta t/2)}, \tag{2.12}$$

where

$$-iC = [(iL_1 + 2iL_2),[iL_1,iL_2]]. \tag{2.13}$$

Here $[\cdots,\cdots]$ denotes the Lie bracket or commutator. The disadvantage of using such a higher order integrator is that the commutator will bring in derivatives of the force with respect to position which may be difficult to calculate.

A. Examples of simple reversible integrators

Consider the propagator generated by the subdivision,

$$iL_2 = \dot{x}\frac{\partial}{\partial x}; \quad iL_1 = F(x)\frac{\partial}{\partial p}. \tag{2.14}$$

This leads to the propagator

$$G(\Delta t) = e^{(\Delta t/2)F(x)\partial/\partial p} e^{\Delta t\dot{x}\partial/\partial x} e^{(\Delta t/2)F(x)\partial/\partial p}. \tag{2.15}$$

Operating with this factorization on $\{x(0),p(0)\}$ and using the explicit property of any operator of the form $e^{c\partial/\partial q}$ that

$$e^{c\partial/\partial q} f(q) = f(q+c), \tag{2.16}$$

where c is independent of q, it is a routine matter to derive the integrator (expressed in terms of positions and velocities),

$$x(\Delta t) = x(0) + \Delta t\dot{x}(0) + \frac{(\Delta t)^2}{2}\frac{F[x(0)]}{m},$$

$$\dot{x}(\Delta t) = \dot{x}(0) + \frac{\Delta t}{2m}\{F[x(0)] + F[x(\Delta t)]\}. \tag{2.17}$$

This is identical to the velocity Verlet algorithms.[10] Because $G(-t) = G^{-1}(t)$, it follows that this integrator is exactly time reversible. This guarantees stability of this integrator and also allows it to be used in the hybrid Monte Carlo algorithm.[4,5,11]

Another way to write this integrator is

$$\dot{x}\left(\frac{\Delta t}{2}\right) = \dot{x}(0) + \frac{\Delta t}{2m}F[x(0)],$$

$$x(\Delta t) = x(0) + \Delta t\dot{x}\left(\frac{\Delta t}{2}\right),$$

$$\dot{x}(\Delta t) = \dot{x}\left(\frac{\Delta t}{2}\right) + \frac{\Delta t}{2m}F[x(\Delta t)]. \tag{2.18}$$

Starting from the initial condition $\{x(0),p(0)\}$ one computes the velocity at the half-step, then the position at the full step, and finishes by calculating the velocity at the full step. This looks like leapfrog, but in practice it is different. In the leapfrog method one initiates the process differently, does not calculate the velocities at the full steps, and only in some cases calculates the last velocity at the full step.

It seems that the most common integrator used in simulations, the Verlet algorithm, cannot be derived using this formalism. However, it can be shown that standard Verlet gives exactly the same trajectory as velocity Verlet. The standard Verlet equations of motion are

$$x(\Delta t) = 2x(0) - x(-\Delta t) + \frac{\Delta t^2}{m}F[x(0)],$$

$$\dot{x}(0) = \frac{x(\Delta t) - x(-\Delta t)}{2\Delta t}. \tag{2.19}$$

If the initial condition is assumed to be

$$x(0) - x(-\Delta t) = \dot{x}(0) - \frac{\Delta t^2}{2m}F[x(0)], \tag{2.20}$$

then it can be shown by induction that the solution obtained by iterating these equations to time t, $\{x(t),\dot{x}(t-\Delta t)\}$ will be equal to that obtained from the velocity Verlet algorithm with initial conditions $\{x(0),\dot{x}(0)\}$. Equivalently, the standard Verlet equations of motion can be obtained from those of velocity Verlet using time reversal symmetry and eliminating the velocities. However, Eq. (2.20) is much more useful as it can be used to convert all the algorithms derived in this paper to the standard Verlet form, as is demonstrated in the Appendix. A similar analysis is possible for leapfrog Verlet, but this is much less widely used and we omit it.

Interestingly, we can generate another reversible algorithm by taking

$$iL_1 = \dot{x}\frac{\partial}{\partial x}; \quad iL_2 = F(x)\frac{\partial}{\partial p}. \tag{2.21}$$

Applying Eq. (2.11) with this subdivision to $\Gamma(0)$ gives

$$\dot{x}(\Delta t) = \dot{x}(0) + \Delta t F\left[x(0) + \frac{\Delta t}{2m}\dot{x}(0)\right],$$

$$x(\Delta t) = x(0) + \frac{\Delta t}{2}[\dot{x}(0) + \dot{x}(\Delta t)]. \tag{2.22}$$

This is an entirely new reversible integrator which we name the *position Verlet* integrator. We will compare it to the velocity Verlet integrator later.

It should be clear from the foregoing that both of these algorithms are of order Δt^3 and that the Trotter factorization is an excellent method for inventing new algorithms. Higher order factorizations should generate higher order reversible algorithms.[6]

B. Numerical comparison of the velocity and position Verlet integrators

To compare the velocity and position Verlet integrators of Eqs. (2.17) and (2.22), respectively, we choose a pure Lennard-Jones (12–6) fluid with 864 particles. The reduced temperature of the system is $\hat{T} = 2.0$ and the reduced density is $\rho\sigma^3 = 1.0$. The potential is cutoff at $r_c = 3\sigma$. The comparison is made by studying the energy conservation as a function of time step Δt for a run whose real time is $N\Delta t$. This energy conservation is defined to be

$$\Delta\hat{E}(\Delta t) = \frac{1}{N}\sum_{k=1}^{N}\left|\frac{E(k\Delta t) - E(0)}{E(0)}\right|. \tag{2.23}$$

A value of $N\Delta t = 1.0$ is chosen and kept the same for all runs. Thus for the two integrators, we solve the classical equations of motion and measure the energy conservation as a function of time step. In Fig. 1, we plot the dependence of $\Delta\hat{E}$ on Δt for the two integrators. The result is very interesting. The curve shows that the velocity Verlet integrator is better at small time steps, but that it becomes unstable more quickly than the position Verlet integrator. For energy conservation tolerances acceptable for typical molecular dynamics calculations, it seems that the velocity Verlet integrator is superior. However, for stability at large time steps, the position Verlet seems better and would thus be a suitable integrator for hybrid Monte Carlo calculations.

C. Reversible algorithms based on generalized Trotter factorizations

It is well known that the Trotter factorization can be generalized to a sum of operators. If the Liouvillian takes the form

$$iL = \sum_{k=1}^{n} iL_k \tag{2.24}$$

then the propagator can be expressed as

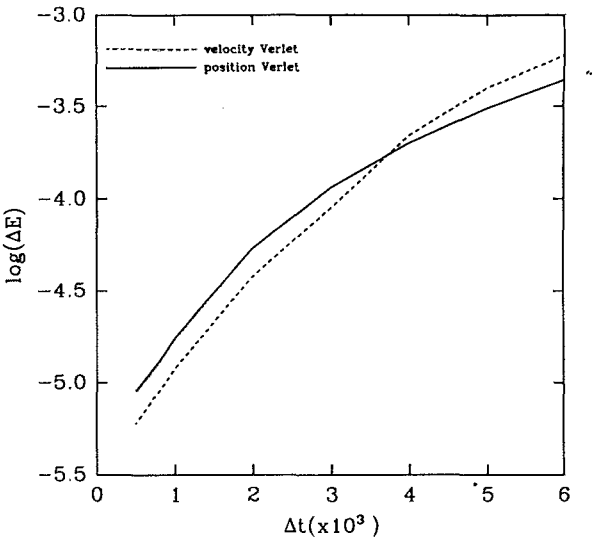

FIG. 1. Comparison of the energy conservation dependence on time step as given by Eq. (2.1) for the velocity Verlet (dashed line) and position Verlet (bold line) integrators for the LJ(12–6) potential.

$$e^{iLt} = \left\{\left[\prod_{k=1}^{n-1} U_k(\Delta t/2)\right]U_n(\Delta t) \times\left[\prod_{k=1}^{n-1} U_{n-k}(\Delta t/2)\right]\right\}^P + O(t^3/P^2), \tag{2.25}$$

where $U_k(h) = e^{iL_k h}$ and $\Delta t = t/P$. Let us define

$$G(\Delta t) = \left[\prod_{k=1}^{n-1} U_k(\Delta t/2)\right]U_n(\Delta t) \times\left[\prod_{k=1}^{n-1} U_{n-k}(\Delta t/2)\right]. \tag{2.26}$$

It is a simple matter to show that $G(\Delta t)$ gives rise to a reversible algorithm given that for each $U_k(\Delta t)$

$$U_k^{\dagger}(\Delta t) = U_k^{-1}(\Delta t) = U_k(-\Delta t) \tag{2.27}$$

(i.e., each L_k is Hermitian). Thus $G(\Delta t)G(-\Delta t) = 1$, and $G(\Delta t)$ generates reversible dynamics.

III. REVERSIBLE REFERENCE SYSTEM PROPAGATOR ALGORITHM (RESPA) FOR SYSTEMS WITH SHORT AND LONG RANGE FORCES

We have previously introduced RESPA[3,12] for accelerating the integration of the equations of motion for systems with forces, $F(x)$, that can be decomposed into short, $F_s(x)$, and long range forces $F_l(x)$ according to

$$F(x) = F_s(x) + F_l(x). \tag{3.1}$$

The short range force then determines the time step δt. In standard methods the full force must be recomputed at the end of each time step. In the RESPA method, however, the short range force is computed after each time step and the long range force is computed every n time steps. This reduces the number of forces calculated and thereby reduces the CPU time. The decomposition of the forces is accomplished by introducing a switching function $S(x)$ that switches from

1 to 0 at some interatomic distance chosen to minimize the CPU time. Then

$$F(x) = S(x)F(x) + [1 - S(x)]F(x) \tag{3.2}$$

and we make the identification

$$F_s(x) = S(x)F(x),$$
$$F_l(x) = [1 - S(x)]F(x). \tag{3.3}$$

In our original formulation we took the reference system to be the dynamical system with only short range forces $F_s(x)$. This was solved numerically for n time steps $\delta t \equiv \Delta t/n$. The equations of motion for the deviations of the reference system from the real system was then solved only once for the time step Δt. This algorithm is not reversible in time. The Trotter factorization allows us to make this strategy reversible.

The basic idea is to define the short range force $F_s(x)$ as a reference system force and to rewrite the Liouville operator as

$$iL = \dot{x}\frac{\partial}{\partial x} + F_s(x)\frac{\partial}{\partial p} + F_l(x)\frac{\partial}{\partial p}$$
$$= iL_s + F_l(x)\frac{\partial}{\partial p}. \tag{3.4}$$

The propagator $e^{iL\Delta t}$ can now be factorized as,

$$G_{lsl}(\Delta t) = e^{(\Delta t/2)F_l(x)\partial/\partial p} e^{iL_s\Delta t} e^{(\Delta t/2)F_l(x)\partial/\partial p}. \tag{3.5}$$

The middle propagator generates motion using the short range forces. Using the Trotter factorization

$$e^{iL_s\Delta t} = [e^{(\delta t/2)F_s(x)\partial/\partial p} e^{\delta t\dot{x}\partial/\partial x} e^{(\delta t/2)F_s(x)\partial/\partial p}]^n, \tag{3.6}$$

where $\delta t = \Delta t/n$ and n is chosen to guarantee stable dynamics. This gives a good approximation to the middle propagator. The propagators on each end of Eq. (3.5) involve the slowly varying long range force and thus will be well approximated as shown with large time step $\Delta t = n\delta t$.

These factorizations give the overall propagator

$$G_{lsl}(\Delta t) = e^{(\Delta t/2)F_l(x)\partial/\partial p}[e^{(\delta t/2)F_s(x)\partial/\partial p} \times e^{\delta t\dot{x}\partial/\partial x} e^{(\delta t/2)F_s(x)\partial/\partial p}]^n e^{(\Delta t/2)F_l(x)\partial/\partial p} \tag{3.7}$$

Examination of Eq. (3.7) reveals that because the long range force propogators correct only the velocities, the long range force as well as the short range force from the previous step carry over as input to the next step. Thus one long range force evaluation and n short range force evaluations will be required in a large time step Δt. There is therefore no more work required for this reversible propogator than for the corresponding nonreversible RESPA method previously introduced.[3] When applied to the initial state $\{x(0),p(0)\}$, this propagator generates the solution (expressed in terms of positions and velocities)

$$x(\Delta t) = x_s\left\{\Delta t; x(0), \dot{x}(0) + \frac{\Delta t}{2m}F_l[x(0)]\right\},$$
$$\dot{x}(\Delta t) = \dot{x}_s\left\{\Delta t; x(0), \dot{x}(0) + \frac{\Delta t}{2m}F_l[x(0)]\right\} + \frac{\Delta t}{2}F_l[x(\Delta t)]. \tag{3.8}$$

In these equations $x_s\{\Delta t; x(0), \dot{x}(0) + (\Delta t/2m)F_l[x(0)]\}$ and $\dot{x}_s\{\Delta t; x(0), \dot{x}(0) + (\Delta t/2m)F_l[x(0)]\}$ denote the solutions of the short range force subject to the initial conditions $\{x(0), \dot{x}(0) + (\Delta t/2m)F_l[x(0)]\}$. The full factorization above dictates that x_s and $\dot{x}_s$ are to be determined numerically using the velocity Verlet integrator [see Eq. (2.17)] iteratively for n small time steps of size δt subject to the initial conditions $\{x(0), \dot{x}(0) + (\Delta t/2m)F_l[x(0)]\}$.

The factorization in Eq. (3.7) is implemented as follows:

(a) Starting with the initial state $\{x(0),p(0)\}$ generate the motion using the propagator $e^{(\Delta t/2)F_l\partial/\partial p}$. This gives the state $\{x(0), p(0) + (\Delta t/2)F_l[x(0)]\}$.

(b) Using the final state of step (a) as the initial state, generate the motion using the middle propagator in Eq. (3.7). This is equivalent to using the velocity Verlet integrator iteratively n times on the system with only short range forces F_s.

(c) Starting with state generated in (b) as the initial state, generate the motion using $e^{(\Delta t/2)F_l\partial/\partial p}$. This gives the final state Eq. (2.11).

In Appendix A, we show to convert this scheme to one which is based on standard Verlet. In Appendix B, we show a few lines of FORTRAN code to illustrate how the algorithm of Eq. (3.8) is implemented in a typical program.

The same treatment can be applied to the factorization given by Eq. (3.8)

$$G_{sls}(\Delta t) = e^{iL_s(\Delta t/2)} e^{\Delta t F_l\partial/\partial p} e^{iL_s(\Delta t/2)}, \tag{3.9}$$

but we shall not do so here because it leads to more computational effort in calculating the potential energy at each step than does the previous factorization. In addition, the position Verlet integrator Eq. (2.22) could have been used in place of the velocity Verlet integrator. Thus there are eight possible factorizations, of which we only discuss one.

A system with long and short range forces. To compare reversible RESPA with nonreversible RESPA, we look at a system studied in our previous work.[3] The system is a LJ(12–6) fluid with a cutoff at $r_c = 3\sigma$ in a box containing 864 particles at a reduced temperature $\hat{T} = 1.0$ and a reduced density $\rho\sigma^3 = 0.8$. For the nonreversible RESPA as outlined in Ref. 3, we study only the reference systems given in Eq. (2.2) of Ref. 3. That is, we let the reference force be simply $F_s(x)$. In all comparisons, we make use of switching function discussed in our previous publications,[3,12] with an inner cutoff of 1.9σ. For reversible RESPA, we use the integration scheme of Eq. (3.8). These two methods are compared with each other and with ordinary velocity Verlet. We study the dependence of energy conservation on Δt according to Eq. (2.1) using $N\Delta t = 1.0$ for all runs. δt is fixed at 1.0×10^{-3}. In Fig. 2 we show the plot of $\Delta\hat{E}$ vs Δt for the three integration methods. We note that reversible RESPA

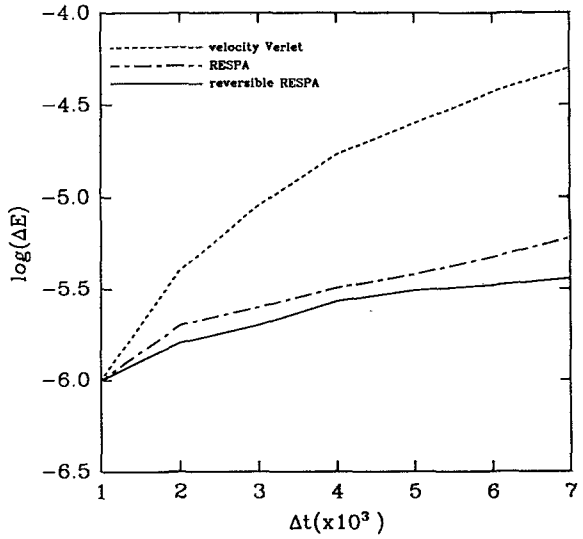

FIG. 2. Comparison of the energy conservation dependence on time step as given by Eq. (2.1) for straightforward velocity Verlet (dashed line), nonreversible RESPA (double dashed line), and reversible RESPA of Eq. (3.7) (bold line) for the long range force breakup.

and nonreversible RESPA agree well at small time steps, but that reversible RESPA is more stable at large time steps. This is to be contrasted with velocity Verlet for which the energy conservation degrades rapidly at large time steps. To quantify this, if we wanted to conserve energy to within a tolerance of $\Delta\widehat{E} = 5\times10^{-6}$, we see from the figure that a time step of 2×10^{-3} would be required for velocity Verlet, while nonreversible RESPA would use a time step of 6×10^{-3} with $n = 6$, and for reversible RESPA, a time step larger than 8×10^{-3} with n around 8 could be used. From our previous work on long range forces,[3] we predict that the CPU savings would be a factor of roughly 3 for nonreversible RESPA and around 4 for reversible RESPA.

IV. REVERSIBLE REFERENCE SYSTEM PROPAGATOR ALGORITHM FOR SYSTEMS WITH MULTIPLE TIME SCALES

We have previously introduced methods for accelerating the integration of the equations of motion for systems with two or more time scales.[1,2] Examples are systems consisting of high frequency oscillators coupled to low frequency oscillators or slow baths,[1] and systems consisting of massive (slow moving) particles interacting with light (fast moving) particles, the so-called disparate mass problem.[2] These methods are based on defining a reference system for the "fast subsystem," solving this either analytically or numerically for a sequence of small time steps, deriving equations of motions for the deviations from the exact trajectory, and then solving the equations of motion for this deviation and for the slow degrees of freedom numerically using a much larger time step. When the reference system is solved numerically the method is called RESPA (reference system propagator algorithm), whereas when it is solved analytically the method is called NAPA (numerical analytical propagator algorithm). These methods reduce the number of forces that must be calculated and thus reduce the CPU time. As we shall see below these methods are not analytically reversible. The Trotter factorization of the propagator allows us to make this strategy reversible and higher order in time.

A. Disparate mass systems

Consider the case where the degrees of freedom of the system can be subdivided into fast and slow degrees of freedom labeled x and y, respectively. An example is[2] that of a binary mixture in which one of the components consists of heavy particles (the y subsystem) and the other component consists of light particles (the x subsystem). Then we can decompose the Liouvillian as

$$iL = iL_x + iL_y, \tag{4.1}$$

where

$$iL_x = \dot{x}\frac{\partial}{\partial x} + F_x(x,y)\frac{\partial}{\partial p_x}, \tag{4.2}$$

$$iL_y = \dot{y}\frac{\partial}{\partial y} + F_y(x,y)\frac{\partial}{\partial p_y}. \tag{4.3}$$

The propagator can thus be factorized as

$$G_{xyx}(\Delta t) = e^{iL_x(\Delta t/2)}e^{iL_y\Delta t}e^{iL_x(\Delta t/2)}. \tag{4.4}$$

For this G_{xyx} factorization the end propagators involve the fast motion whereas the middle propagator involves the slow motion. Although is it not as obvious as in the long range force case [Eq. (3.7)], these factorization involves the same number of force evaluations as does the nonreversible disparate mass RESPA method previously introduced.[2] This follows from the fact that $F_{xy} = -F_{yx}$, so that this part of the force need only be calculated while advancing the fast coordinate. The fast propagator can be further factorized

$$e^{iL_x(\Delta t/2)} = [e^{(\delta t/2)F_x\partial/\partial p_x}e^{\delta t\dot{x}\partial/\partial x}e^{(\delta t/2)F_x\partial/\partial p_x}]^{n/2}, \tag{4.5}$$

where $\delta t = \Delta t/n$. The middle propagator in G_{xyx} can also be factorized, but because it involves only the slow motion we can use

$$e^{iL_y\Delta t} = e^{(\Delta t/2)F_y\partial/\partial p_y}e^{\Delta t\dot{y}\partial/\partial y}e^{(\Delta t/2)F_y\partial/\partial p_y}. \tag{4.6}$$

If these factorizations are used in Eq. (4.4) the fast degrees of freedom and their conjugate momenta $\{x,p_x\}$ are to be determined numerically using the velocity Verlet integrator [see Eq. (2.17)] iteratively for n small time steps δt subject to whatever the initial conditions might be, whereas the slow degrees of freedom are to be determined using the velocity Verlet integrator for only one large step Δt.

We can summarize the numerical procedure that follows from application of G_{xyx} as follows:

(a) Use the velocity Verlet integrator for $n/2$ time steps $\delta t = \Delta t/n$ to generate the state at time $\Delta t/2$ under the action of the the propagator $e^{iL_x\Delta t/2}$ starting from the initial state $\{x(0),y(0),p_x(0),p_y(0)\}$. Note that during this step $\{y,p_y\}$ is unchanged.

(b) Use the velocity Verlet integrator for one time step Δt to advance the system from the final state of step (a) using the slow propagator Eq. (4.6).

(c) Use the velocity Verlet integrator for $n/2$ time steps

$\delta t = \Delta t/n$ to generate the state at time $\Delta t/2$ under the action of the propagator $e^{iL_x \Delta t/2}$, starting from the final state in (b). Note that during this step $\{y,p_y\}$ is again held fixed. The resulting state is $\Gamma(\Delta t)$.

In the foregoing the forces on the slow coordinates are recalculated only once every time step, $\Delta t = n\delta t$. If the dimensionality of the fast subsystem is small compared to the dimensionality of the whole system, the forces on the slow coordinates will thus be calculated much less frequently than would be required in the standard methods.

There are many variations on the above theme. For example, we could have adopted the Trotter factorization

$$G_{yxy} = e^{iL_y(\Delta t/2)} e^{iL_x \Delta t} e^{iL_y(\Delta t/2)} \tag{4.7}$$

and then applied the velocity Verlet breakups. Alternatively, we could use the position Verlet integrator instead of the velocity Verlet factorizations of the different factors in G_{xyx} or G_{yxy}. There are eight possibilities in all. For the purposes of the subsequent discussion, we look only at G_{xyx} with the velocity Verlet [see Eq. (2.17)] breakup applied to each of the factors in G_{xyx}.

Numerical comparison for the disparate mass system. The comparison of reversible RESPA to nonreversible RESPA proceeds now on a system studied in our previous work.[2] Again, we look at a system of LJ(12–6) particles this time at reduced temperature $\hat{T} = 0.67$ and reduced density $\rho\sigma^3 = 0.86$, which correspond to the triple point. Again, the potential is cutoff at $r_c = 3\sigma$. The system is comprised of a mixture of 40 light ($m = 1$) particles and 824 heavy ($M = 100$) particles. The nonreversible RESPA simulations are carried out as described in Ref. 2 in which the reference force is taken to be $F_r(x) = F_x[x,y(0)]$, whereas the reversible RESPA simulations are done using the propagator of Eq. (4.4). When this propagator is used the explicit algorithm for advancing the positions and velocities is given by

$$\begin{aligned} x(\Delta t) &= x_r\left(\frac{\Delta t}{2}; x_0, \dot{x}_0, y_0\right), \\ \dot{x}(\Delta t) &= \dot{x}_r\left(\frac{\Delta t}{2}; x_0, \dot{x}_0, y_0\right), \\ y(\Delta t) &= y_r[\Delta t; y(0), \dot{y}(0), x_0], \\ \dot{y}(\Delta t) &= y_r[\Delta t; y(0), \dot{y}(0), x_0], \end{aligned} \tag{4.8}$$

where

$$\begin{aligned} x_0 &= x_r\left[\frac{\Delta t}{2}; x(0), \dot{x}(0), y(0)\right], \\ \dot{x}_0 &= \dot{x}_r\left[\frac{\Delta t}{2}; x(0), \dot{x}(0), y(0)\right], \end{aligned} \tag{4.9}$$

x_r and y_r refer to the evolution of x and y under the actions of $e^{iL_x t}$ and $e^{iL_y t}$, respectively. The velocity Verlet breakup of Eq. (2.17) is applied to the propagators $e^{iL_x t}$ and $e^{iL_y t}$. In all simulations, the light (x) particles are integrated using $\delta t = \Delta t/10$. The energy conservation is measured as before using Eq. (2.1) and $\hat{T}$ is chosen equal to 1.0. In Fig. 3, we show the plot of $\Delta\hat{E}$ vs Δt. Figure 3 shows that while nonreversible RESPA is consistently better than velocity Verlet, reversible RESPA is dramatically better and remains remarkably stable even at large time steps. While velocity Verlet becomes unstable at $\Delta t = 0.04$, the energy conservation for reversible RESPA is better than 10^{-5}, and for nonreversible RESPA it is better than 5×10^{-5}. In Fig. 4, we plot the

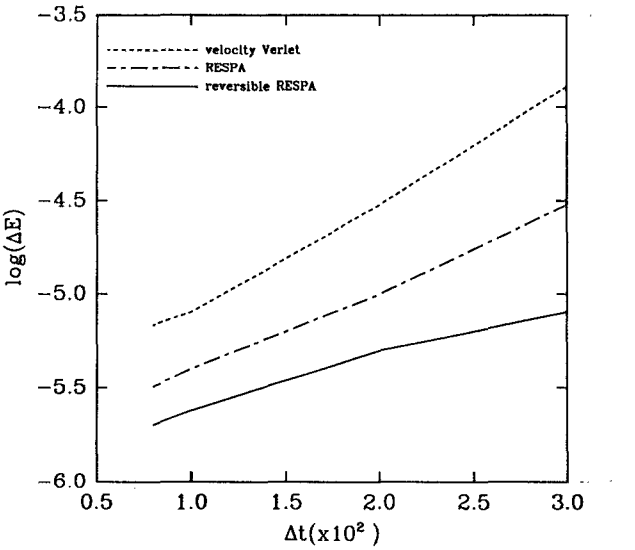

FIG. 3. Comparison of the energy conservation dependence on time step as given by Eq. (2.1) for straightforward velocity Verlet (double dashed line), nonreversible RESPA (dashed line), and the disparate mass breakup of Eq. (4.4) (bold line).

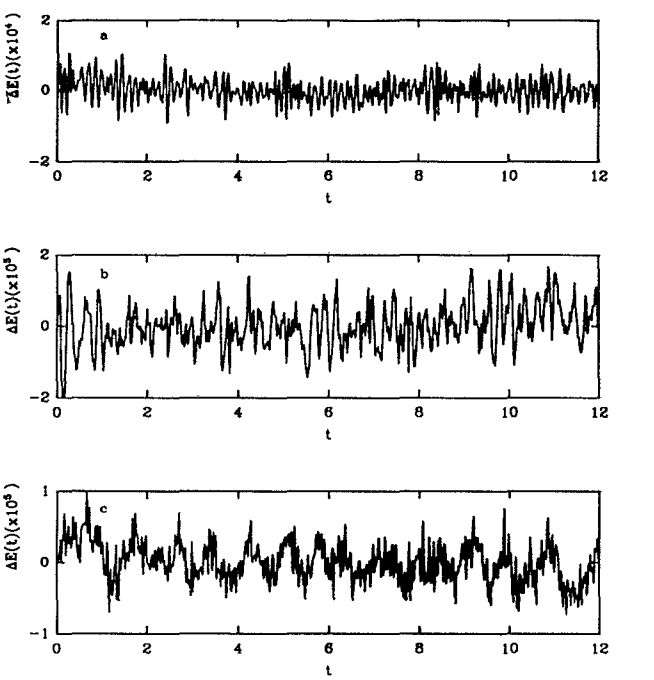

FIG. 4. (a) The instantaneous fluctuations of the energy about $E(0)$ for velocity Verlet in the disparate mass system at a time step $\Delta t = 2\times10^{-2}$. (b) The same except for nonreversible RESPA. (c) The same except for reversible RESPA.

instantaneous fluctuations of the energy about the initial value. That is, we plot

$$\Delta E(t) = \frac{E(t) - E(0)}{E(0)} \qquad (4.10)$$

for each of the three integrators for a time step of $\Delta t = 2 \times 10^{-2}$. In Fig. 3, this corresponds to an average energy conservation of about 3×10^{-5} for velocity Verlet, 1×10^{-5} for nonreversible RESPA, and 3×10^{-6} for reversible RESPA. From these plots, we can determine the maximum of the fluctuations, and discern whether or not the system has a systematic drift. Although the behavior of the instantaneous fluctuations is different in each of the three cases, we see that they are all stable at this time step.

B. A stiff oscillator dissolved in a soft liquid

Another kind of system of interest is that of a stiff oscillator with vibrational coordinate labeled x buried in a soft bath with coordinates labeled y. For convenience we will also consider the center of mass coordinate of the oscillator as well as its orientational coordinates as part of the bath.

It is possible to break the force $F_x(x,y)$ on the vibrational degree of freedom into a strong, possibly analytically solvable force, and a weak correction. The basic idea is to define a reference system force $F_r(x)$ and to rewrite the Liouville operator as

$$iL = \dot{x}\frac{\partial}{\partial x} + F_r(x)\frac{\partial}{\partial p_x} + f(x,y)\frac{\partial}{\partial p_x} + \dot{y}\frac{\partial}{\partial y} + F_y(x,y)\frac{\partial}{\partial p_y}, \qquad (4.11)$$

where $f(x,y) = F_x(x,y) - F_r(x)$. f contains forces on x due to the solvent atoms. This allows us to subdivide the Liouvillian into parts

$$iL_r = \dot{x}\frac{\partial}{\partial x} + F_r(x)\frac{\partial}{\partial p_x} \qquad (4.12)$$

and

$$iL_y = \dot{y}\frac{\partial}{\partial y} + F_y(x,y)\frac{\partial}{\partial p_y} + f(x,y)\frac{\partial}{\partial p_x}. \qquad (4.13)$$

The propagator $e^{iL\Delta t}$ can now be factorized as

$$G_{yry}(\Delta t) = e^{iL_y(\Delta t/2)} e^{iL_r\Delta t} e^{iL_y(\Delta t/2)} \qquad (4.14)$$

or

$$G_{ryr}(\Delta t) = e^{iL_r(\Delta t/2)} e^{iL_y\Delta t} e^{iL_r(\Delta t/2)}. \qquad (4.15)$$

Factorization of the middle propagator in Eq. (4.14) as

$$e^{iL_r\Delta t} = \left[e^{(\delta t/2)F_x\partial/\partial p_x} e^{\delta t\dot{x}\partial/\partial x} e^{(\delta t/2)F_x\partial/\partial p_x}\right]^n, \qquad (4.16)$$

where $\delta t = \Delta t/n$. If the reference system can be solved analytically (e.g., a harmonic, cubic, or Morse oscillator) then the above factorization is not necessary. A simple way to include the solvent effects into the full propagator yields the following result for $G_{yry}(\Delta t)$:

$$G(\Delta t) = e^{(\Delta t/2)F_y(x,y)\partial/\partial p_y} e^{(\Delta t/2)f(x,y)\partial/\partial p_x} e^{(\Delta t/2)\dot{y}\partial/\partial y} \times e^{iL_r\Delta t} e^{(\Delta t/2)\dot{y}\partial/\partial y} e^{(\Delta t/2)f(x,y)\partial/\partial p_x} \times e^{(\Delta t/2)F_y(x,y)\partial/\partial p_y}. \qquad (4.17)$$

Using this factorization of the propagator, the integration procedure generated in terms of positions and velocities is

$$x(\Delta t) = x_r\left[\Delta t; x(0), \dot{x}(0) + \frac{\Delta t}{2m}f(0)\right],$$

$$\dot{x}(\Delta t) = \dot{x}_r\left[\Delta t; x(0), \dot{x}(0) + \frac{\Delta t}{2m}f(0)\right] + \frac{\Delta t}{2m}f(\Delta t),$$

$$y(\Delta t) = y(0) + \Delta t\dot{y}(0) + \frac{\Delta t^2}{2m}F_y(0),$$

$$\dot{y}(\Delta t) = \dot{y}(0) + \frac{\Delta t}{2m}[F_y(0) + F_y(\Delta t)]. \qquad (4.18)$$

This particular factorization has the obvious simplicity that the solvent is integrated using velocity Verlet. This breakup is a generalization of the Trotter form as discussed in Sec. II C. The same treatment can be applied to the factorization given by Eq. (4.15) but we shall not do so here.

Numerical comparisons for a stiff oscillator in a soft fluid. The comparison between reversible and nonreversible RESPA proceeds, as before, on a system considered in our previous work.[1] We look at a system of 62 LJ(12–6) particles in which is imbedded a high frequency harmonic oscillator. The reduced temperature and density of the liquid are $\hat{T} = 2.5$ and $\rho\sigma^3 = 1.05$. The frequency of the oscillator is taken to be $\omega = 300$. Since the peak of the spectral density of the neat liquid at this density and temperature is around $\omega = 20$, the oscillator frequency $\omega = 300$ is an extremely high frequency. Since the reference force $F_r(x) = -m\omega^2 x^2$ is harmonic, we can evaluate the action of the reference system propagator analytically in the usual way as

$$e^{iL_r\Delta t}x = x\cos\omega\Delta t + \frac{\dot{x}}{\omega}\sin\omega\Delta t,$$

$$e^{iL_r\Delta t}\dot{x} = \dot{x}\cos\omega\Delta t - \omega x\sin\omega\Delta t. \qquad (4.19)$$

We follow the evolution of the system for 500 periods of the oscillator using ordinary velocity Verlet, NAPA, and reversible NAPA. The result of the comparison of the three integrators is shown in Fig. 5 in which is plotted the energy conservation vs Δt as in Eq. (2.1). We see that the reversible NAPA as given by Eq. (4.18) is highly accurate at all time steps, while the nonreversible NAPA tends to become significantly less accurate than reversible NAPA for time steps greater than about 10^{-3}. This is due to the fact that nonreversible NAPA, being less stable than reversible NAPA. However, since both NAPA methods are based on analytically solvable stiff reference systems we expect them to agree well at smaller time steps, which they do. The extreme stiffness of the reference system illustrates the advantage of using a reference system algorithm over ordinary velocity Verlet

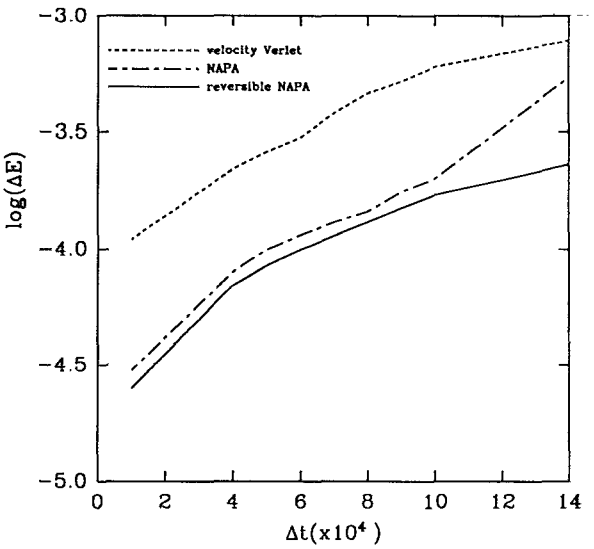

FIG. 5. Comparison of the energy conservation dependence on time step as given by Eq. (2.1) for straightforward velocity Verlet (double dashed line), nonreversible NAPA (dashed line), and the reversible NAPA scheme of Eq. (4.17) (bold line) for the stiff oscillator dissolved in a soft solvent.

which is significantly less accurate than NAPA or reversible NAPA for reasonable energy conservation tolerances (10^{-3}–10^{-4} or better).

V. SYSTEMS WITH SEPARATION OF TIME SCALES AND SHORT AND LONG RANGE FORCES

In the foregoing we have treated systems in which forces can be subdivided into short and long range components. Reference system methods lead to a considerable saving in CPU time. We have also discussed systems in which there is a large separation in time scales such as stiff oscillators embedded in soft fluids or disparate mass systems. In systems with separation of time scales and with force fields that can be decomposed into short and long range forces it is possible to devise reference system methods that can accelerate the solution of the equations of motion. In a previous publication we were able to apply a double reference system approach (double RESPA) to greatly accelerate such systems. This method was not reversible. Here we show how one can generate reversible multiple RESPA procedures to handle systems like these.

The propagator for the disparate mass system given in Eq. (4.4) can be expressed as

$$G_{xyx}(\Delta t) = G_{lsl}^{(x)}\left(\frac{\Delta t}{2}\right) G_{lsl}^{(y)}(\Delta t) G_{lsl}^{(x)}\left(\frac{\Delta t}{2}\right), \quad (5.1)$$

where

$$G_{lsl}^{(x)}(\Delta t) = e^{(\Delta t/2)F_{xl}(x,y)\partial/\partial p_x} e^{iL_{xs}\Delta t} \times e^{(\Delta t/2)F_{xl}(x,y)\partial/\partial p_x} \quad (5.2)$$

and

$$G_{lsl}^{(y)}(\Delta t) = e^{(\Delta t/2)F_{yl}(x,y)\partial/\partial p_y} e^{iL_{ys}\Delta t} \times e^{(\Delta t/2)F_{yl}(x,y)\partial/\partial p_y}. \quad (5.3)$$

The middle propagator in Eq. (5.2) involves the fast degrees of freedom and the short range forces acting on them and can thus be further factorized as in Eq. (4.5), whereas the middle propagator in Eq. (5.3) involves the slow degrees of freedom propagating under the short range forces and can thus be factorized as in Eq. (4.6). The overall propagator then generates a reversible double RESPA algorithm which can lead to enormous savings in CPU times. The extension of this idea to the stiff oscillator problem is straightforward.

VI. REVERSIBLE ALGORITHMS FROM PREDICTOR–CORRECTOR INTEGRATORS

The use of the Liouville operator formalism to derive integrators is a somewhat novel approach. It is, however, satisfying to know that even the standard integrators of molecular dynamics can be obtained from a "first principles" approach. Nevertheless, it is useful to draw the connection between the Liouville operator formalism and the more conventional predictor–corrector scheme.[8,13] In this section we address this issue.

The usual approach in a predictor–corrector scheme is to "predict" the state of the system based on the initial conditions for the current time step, and then to correct the prediction based on the forces evaluated at the predicted positions. We show that the Trotter breakup of the propagator is equivalent to a predictor–corrector scheme. Consider the Trotter breakup of Eq. (2.15) which yields the velocity Verlet

$$e^{iL\Delta t} = e^{(\Delta t/2)F(x)\partial/\partial p} e^{\Delta t\dot{x}\partial/\partial x} e^{(\Delta t/2)F(x)\partial/\partial p}. \quad (6.1)$$

Mathematically, this breakup is equivalent to the following set of equations

$$\frac{dv}{dt} = \frac{1}{m}F(x), \quad (6.2)$$

$$\frac{dx}{dt} = v, \quad (6.3)$$

$$\frac{dv}{dt} = \frac{1}{m}F(x), \quad (6.4)$$

with the prescription that Eq. (6.2) is solved for a half time step $\Delta t/2$, with initial conditions $\{x(0), v(0)\}$ and holding $x(0)$ fixed. This yields the predicted value $v(\Delta t/2) = v(0) + (\Delta t/2m)F(x)$. Then Eq. (6.3) is solved for a full time step using the predicted value of v and $x(0)$ as the initial conditions. This yields the true position $x(\Delta t)$. Finally, we correct the velocities using Eq. (6.4) with initial conditions $x(\Delta t)$ and $v(\Delta t/2)$. Following this procedure will yield the scheme of Eq. (2.18). Reversibility comes from having a symmetric set of equations. The middle step in which x is integrated can be thought of as a reference system integration done analytically, since $e^{\Delta t\dot{x}\partial/\partial x}$ would be the propagator for a reference system with $F_r(x) = 0$. With this in mind, we can easily extend this idea to reversible RESPA.

Now consider the example of a system with long and short range force components. The Trotter expansion of the propagator takes the form given in Eq. (3.7)

$$e^{iL\Delta t} = e^{(\Delta t/2)F_l(x)\partial/\partial p} e^{iL_r\Delta t} e^{(\Delta t/2)F_l(x)\partial/\partial p},$$

where $iL_r = \dot{x}\partial/\partial x + F_s(x)\partial/\partial p$. As above we can cast this into the equivalent form

$$\frac{dv}{dt} = \frac{1}{m}F_l(x), \tag{6.5}$$

$$\frac{dx}{dt} = v,$$

$$\frac{dv}{dt} = \frac{1}{m}F_s(x), \tag{6.6}$$

$$\frac{dv}{dt} = \frac{1}{m}F_l(x). \tag{6.7}$$

The scheme is now transparent. Eq. (6.5) is integrated for a half step $\Delta t/2$ with initial conditions $x(0), v(0)$. This yields the predicted value $v(\Delta t/2) = v(0) + (\Delta t/2m)F_l(0)$. Then Eqs. (6.6) are integrated for a full step Δt using the predicted value $v(\Delta t/2)$ and $x(0)$ as initial conditions. This yields a reference system trajectory in which the position is the true position $x_r(\Delta t) = x(\Delta t)$. Then the reference velocity is corrected by Eq. (6.7) using as initial conditions $x(\Delta t)$ and $v(\Delta t/2)$. As before, reversibility comes from having a symmetric set of equations. It should now be clear how to generate predictor–corrector schemes for other systems with reference forces.

VII. A REVERSIBLE ALGORITHM FOR NOSÉ DYNAMICS

We now discuss integration of systems with multiple time scales obeying Nosé dynamics.[14,15] Recall that Nosé's equations of motion for a system of N particles in virtual variables can be generated from the Hamiltonian

$$H = \sum \frac{p^2}{2ms^2} + V(x) + \frac{p_s^2}{2Q} + (3N+1)kT\ln s. \tag{7.1}$$

The equations of motion derived from this Hamiltonian are

$$\dot{x} = \frac{\partial H}{\partial p} = \frac{p}{ms^2},$$

$$\dot{p} = -\frac{\partial H}{\partial x} = -\frac{\partial V}{\partial x},$$

$$\dot{s} = \frac{\partial H}{\partial p_s} = \frac{p_s}{Q},$$

$$\dot{p}_s = -\frac{\partial H}{\partial s} = \frac{1}{s}\left[\sum \frac{p^2}{ms^2} - (3N+1)kT\right]. \tag{7.2}$$

By introducing the time scaling $dt \to dt/s$ and the change of variables $p \to p/s$, $p_s \to p_s/s$, and introducing as a dynamical variable $\eta = \ln s$, one obtains Nosé–Hoover equations[16]

$$\dot{x} = \frac{p}{m},$$

$$\dot{p} = -\frac{\partial V}{\partial x} - \frac{p_\eta}{Q}p,$$

$$\dot{\eta} = \frac{p_\eta}{Q},$$

$$\dot{p}_\eta = \sum \frac{p^2}{m} - 3NkT. \tag{7.3}$$

Here we have chosen to use the variable $\eta = \int^t \zeta\, dt$ instead of ζ as introduced by Hoover in order to make the equation for η second order.

In order to derive a reversible integrator for the Nosé–Hoover equations, we recognize that these equations can be derived using the Liouville operator[17]

$$iL = \dot{x}\frac{\partial}{\partial x} + F_r(x)\frac{\partial}{\partial p} + f(x)\frac{\partial}{\partial p} - \dot{\eta}p\frac{\partial}{\partial p} + \dot{\eta}\frac{\partial}{\partial \eta} + F_\eta(p)\frac{\partial}{\partial p_\eta}, \tag{7.4}$$

where $F_\eta(p) = \Sigma(p^2/m) - 3NkT$ or $F_\eta(\dot{x}) = \Sigma(m\dot{x}^2) - 3NkT$. We have introduced the reference system force $F_r(x)$ and the deviation of the true force from the reference force $f(x) = F(x) - F_r(x)$. It should be noted that although the conserved energy is

$$H' = \sum \frac{p^2}{2m} + V(x) + \frac{p_\eta^2}{2Q} + (3N+1)kT\eta, \tag{7.5}$$

as can be verified by computing iLH' using Eqs. (7.4) and (7.5), this energy is not a Hamiltonian, and the Liouville operator of Eq. (7.4) cannot be derived from it. However, it can be used in conjunction with Eq. (2.1) to measure how well the integration algorithm conserves the energy. Defining the reference system propagator as $iL_r = \dot{x}\partial/\partial x + F_r(x)\partial/\partial p$, the propagator $e^{iL\Delta t}$ is factorized as

$$\begin{aligned} G(\Delta t) = {} & e^{(\Delta t/2)F_\eta(p)\partial/\partial p_\eta} e^{(\Delta t/4)f(x)\partial/\partial p} e^{-(\Delta t/2)\dot{\eta}p\partial/\partial p} \\ & \times e^{(\Delta t/4)f(x)\partial/\partial p} e^{(\Delta t/2)\dot{\eta}\partial/\partial \eta} e^{iL_r\Delta t} \\ & \times e^{(\Delta t/2)\dot{\eta}\partial/\partial \eta} e^{(\Delta t/4)f(x)\partial/\partial p} e^{-\Delta t/2)\dot{\eta}p\partial/\partial p} \\ & \times e^{(\Delta t/4)f(x)\partial/\partial p} e^{(\Delta t/2)F_\eta(p)\partial/\partial p_\eta}. \end{aligned} \tag{7.6}$$

We act with this propagator on the initial state $[x(0), p(0), \eta(0), p_\eta(0)]$, and use the fact that

$$e^{-(\Delta t/2)\dot{\eta}p\partial/\partial p}\phi(p) = \phi(pe^{-(\Delta t/2)\dot{\eta}}). \tag{7.7}$$

The above identity as well as Eq. (2.16) are special cases of the general identity for the function $e^{c\partial/\partial g(q)}f(q)$,

$$\begin{aligned} e^{c\partial/\partial g(q)}f(q) &= e^{c\partial/\partial g(q)}f\{g^{-1}[g(q)]\} \\ &= f\{g^{-1}[g(q)+c)]\}, \end{aligned} \tag{7.8}$$

where c is independent of q. The result is a reversible integrator for Nosé dynamics,

$$x(\Delta t) = x_r[\Delta t; x(0), \dot{x}_0],$$

$$\dot{x}(\Delta t) = \left\{\dot{x}_r[\Delta t; x(0), \dot{x}_0] + \frac{\Delta t}{4m}f(\Delta t)\right\} \times e^{-(\Delta t/2)\dot{\eta}_0} + \frac{\Delta t}{4m}f(\Delta t),$$

$$\eta(\Delta t) = \eta(0) + \Delta t\dot{\eta}(0) + \frac{\Delta t^2}{2Q}F_\eta[\dot{x}(0)],$$

$$\dot{\eta}(\Delta t) = \dot{\eta}(0) + \frac{\Delta t}{2Q}\{F_\eta[\dot{x}(0)] + F_\eta[\dot{x}(\Delta t)]\}, \quad (7.9)$$

where

$$\dot{x}_0 = \left[\dot{x}(0) + \frac{\Delta t}{4m} f(0)\right] e^{-(\Delta t/2)\dot{\eta}_0} + \frac{\Delta t}{4m} f(0)$$

$$\dot{\eta}_0 = \dot{\eta}(0) + \frac{\Delta t}{2Q} F_\eta[\dot{x}(0)]. \quad (7.10)$$

The simplicity of this integrator is that the bath is integrated with ordinary velocity Verlet, and the dissipative effect of the bath on the system is handled analytically in the $e^{-(\Delta t/2)\dot{\eta}_0}$ terms. We see that this factorization is of a generalized Trotter form as discussed in Sec. II C. In the Appendix, we show how to convert this algorithm to one based on the standard Verlet. Note that it is possible to incorporate the both variables η and P_η into the reference system and define the Liouville operator as

$$iL = f(x)\frac{\partial}{\partial p} + iLr,n, \quad (7.11)$$

where the definition of iLr,n can be inferred from Eq. (7.4). The breakup of the propagator is then

$$G(\Delta t) = e^{(\Delta t/2)f(x)\partial/\partial p} e^{iLr,n\Delta t} e^{(\Delta t/2)f(x)\partial/\partial p} \quad (7.12)$$

Although this tends to be a slower algorithm, it proves to be more stable when multiple Nosé baths are involved and can handle large fluctuations in $\dot{\eta}$ more stably.

Numerical comparisons for Nosé dynamics. The integrator in Eq. (7.9) is compared to straight velocity Verlet on the system considered in Sec. III. That is, we consider a system of 864 LJ(12–6) particles at a temperature 1.0 and density 0.8 using the long range force breakup to define the reference system. The mass of the Nosé particle is $Q = 2.0$ chosen according to the formula $Q = 3NkT\tau^2$, where τ is some characteristic time in the system. Since the forces are velocity dependent, the straight velocity Verlet simulations must be done by iterating the velocity integration step starting with the approximation $\dot{x}_{\text{approx}}(\Delta t) = \dot{x}(0) + \Delta t/m[F(0) - \dot{\eta}(0)\dot{x}(0)]$. Ten iterations of this approximation are used to obtain the final velocity $\dot{x}(\Delta t)$. Figure 6 shows the comparison of energy conservation defined by Eq. (2.1). We see that the reversible RESPA method for Nosé dynamics is a dramatic improvement over straight velocity Verlet and is remarkably stable at large time steps.

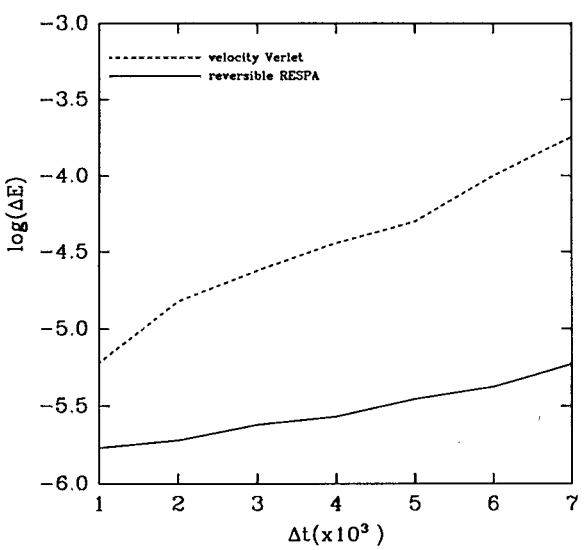

FIG. 6. Comparison of the energy conservation dependence on time step as given by Eq. (2.1) for straightforward velocity Verlet (dashed line), and the reversible RESPA scheme for Nosé dynamics of Eq. (7.6).

VIII. CONCLUSION

Dynamical systems with multiple time scales pose a major problem in simulations because the small time steps required for stable integration of the fast motions lead to large numbers of time steps required for the observation of the slow degrees of freedom and thus to the need to compute a large number of forces. As we have shown in several previous publications, reference system methods (RESPA) greatly reduce the CPU time for the simulation of such systems.[1–3,12,18] In this paper we have used reversible forms of RESPA that are superior to the previous RESPA methods both with respect to the order and stability of the integrators. Moreover, because these are reversible they can also be used in the hybrid Monte Carlo methods.[4,5] We have limited this discussion to a few obvious factorizations of the propagator based on the Trotter factorization, and we have shown how one can use a more general breakup. This procedure is put in the context of predictor–corrector methods and is applied to several different dynamical systems. It is shown how simple factorizations give rise to the velocity Verlet integrator and to a new integrator which we call the position Verlet integrator. It is shown how the problem with multiple time steps like the disparate mass problem and the problem of stiff oscillators in soft baths can be treated. A very important class of problems in which the forces can be subdivided into short and long range forces is treated by these methods. It is shown how to combine these latter two classes of problems with very large speedups. Finally, we incorporate these RESPA methods in the treatment of systems interacting with a Nosé heat bath for constant temperature molecular dynamics. The approach outlined here is easily generalizable to many more integration strategies.

ACKNOWLEDGMENTS

This work was supported by a grant from the National Science Foundation (NSF CHE-87-00522 and by a grant from the National Institutes of Health (GM43340-01A1). One of us (B.J.B.) would like to thank Dr. J. Sexton and Dr. D. Weingarten for discussions about the time reversibility of the Trotter factorization.

APPENDIX A

In this Appendix, we show how to obtain reference system integration schemes based on the standard Verlet algorithm. The strategy is the same as that employed in Eq. (2.20). Thus the starting point for these derivations is the velocity Verlet based integrators.

Consider, first, the case of the long range force integrator discussed in Sec. III. The velocity Verlet based algorithm gave the positions and velocities at each time step to be

$$x(\Delta t) = x_s\left\{\Delta t; x(0), \dot{x}(0) + \frac{\Delta t}{2m} F_l[x(0)]\right\},$$
$$\dot{x}(\Delta t) = \dot{x}_s\left\{\Delta t; x(0), \dot{x}(0) + \frac{\Delta t}{2m} F_l[x(0)]\right\} + \frac{\Delta t}{2} F_l[x(\Delta t)]. \quad \text{(A1)}$$

In standard Verlet, we start with the initial conditions $\{x(0), x(-\delta t)\}$, where $\delta t \equiv \Delta t/n$. Using the condition in Eq. (2.20), the standard Verlet scheme is obtained as follows: First, define

$$x'(-\delta t) = x(-\delta t) - \frac{(\Delta t)(\delta t)}{2m} F_l[x(0)] \quad \text{(A2)}$$

and

$$x'(\delta t) = 2x(0) - x'(-\delta t) + \frac{\delta t^2}{m} F_s[x(0)]. \quad \text{(A3)}$$

Then, we compute the velocity $\dot{x}(0)$ from

$$\dot{x}(0) = \frac{x'(\delta t) - x'(-\delta t)}{2\delta t}. \quad \text{(A4)}$$

Then, by defining

$$x''(-\delta t) = x'(-\delta t) - \frac{(\Delta t)(\delta t)}{2m} F_l[x(0)], \quad \text{(A5)}$$

we obtain the positions at $x(\Delta t - \delta t)$ and $x(\Delta t)$

$$x(\Delta t - \delta t) = x_s[\Delta t - \delta t, x(0), x''(-\delta t)], \quad \text{(A6)}$$
$$x(\Delta t) = x_s[\Delta t, x(0), x''(-\delta t)], \quad \text{(A7)}$$

where $x_s(\tau)$ denotes the solution of the reference system using the standard Verlet algorithm for p steps where $p = \tau/\delta t$ subject to the initial conditions $\{x(0), x''(-\delta t)\}$. The need for both $x(\Delta t - \delta t)$ and $x(\Delta t)$ is clear from the initial conditions required to initiate each step.

As a final example, we show how to obtain the standard Verlet scheme for Nosé dynamics as discussed in Sec. VII. For simplicity, we consider the case of $F_r(x) = F(x)$ although generalization to a different reference force is straightforward. The initial conditions are given as $\{x(0), x(-\Delta t), \eta(0), \eta(-\Delta t)\}$. Again, using the condition in Eq. (2.20), we define

$$x'(-\Delta t) = e^{-(\Delta t/2)\dot{\eta}_0(-\Delta t)} x(-\Delta t) + [1 - e^{-(\Delta t/2)\dot{\eta}_0(-\Delta t)}] \times \left[x(0) + \frac{\Delta t^2}{2m} F(0)\right] \quad \text{(A8)}$$

and

$$x'(\Delta t) = 2x(0) - x'(-\Delta t) + \frac{\Delta t^2}{m} F(0). \quad \text{(A9)}$$

The velocity $\dot{x}(0)$ is then obtained from

$$\dot{x}(0) = \frac{x'(\Delta t) - x'(-\Delta t)}{2\Delta t}. \quad \text{(A10)}$$

The evolution of the bath coordinate is given by the usual Verlet scheme

$$\eta(\Delta t) = 2\eta(0) - \eta(-\Delta t) + \frac{\Delta t^2}{2Q} F_\eta(0), \quad \text{(A11)}$$

$$\dot{\eta}(0) = \frac{\eta(\Delta t) - \eta(-\Delta t)}{2\Delta t}. \quad \text{(A12)}$$

Finally, to evolve the system coordinate x, we define

$$x''(-\Delta t) = e^{-(\Delta t/2)\dot{\eta}_0(0)} x'(-\Delta t) + [1 - e^{-(\Delta t/2)\dot{\eta}_0(0)}] \times \left[x(0) + \frac{\Delta t^2}{2m} F(0)\right] \quad \text{(A13)}$$

from which, we obtain the position $x(\Delta t)$

$$x(\Delta t) = 2x(0) - x''(-\Delta t) + \frac{\Delta t^2}{m} F(0). \quad \text{(A14)}$$

In the above, η_0 is defined in Eq. (7.10).

APPENDIX B

The following is a piece of FORTRAN code which shows how to implement the integration algorithm expressed in Eq. (3.8). These lines of code assume that the long and short range force components are known from a previous integration step. *dt_long* is the big time step Δt in Eq. (3.8), while *dt_short* corresponds to the small time step δt with which the reference system is integrated. *Ninner* is the number of small time steps per big time step.

```
DO i = 1,Natoms
VX(i) = VX(i) + 0.5*dt_long*FX_long(i)
VY(i) = VY(i) + 0.5*dt_long*FY_long(i)
VZ(i) = VZ(i) + 0.5*dt_long*FZ_long(i)
ENDDO
DO inner = 1, Ninner
DO i = 1,Natoms
X(i) = X(i) + dt_short*VX(i) + 0.5
          *dt2_short*FX_short(i)
Y(i) = Y(i) + dt_short*VY(i) + 0.5
          *dt2_short*FY_short(i)
Z(i) = Z(i) + dt_short*VZ(i) + 0.5
          *dt2_short*FZ_short(i)
VX(i) = VX(i) + 0.5*dt_short*FX_short(i)
VY(i) = VY(i) + 0.5*dt_short*FY_short(i)
VZ(i) = VZ(i) + 0.5*dt_short*FZ_short(i)
ENDDO

CALL FORCES_short
DO i = 1,Natoms
VX(i) = VX(i) + 0.5*dt_short*FX_short(i)
VY(i) = VY(i) + 0.5*dt_short*FY_short(i)
VZ(i) = VZ(i) + 0.5*dt_short*FZ_short(i)
ENDDO
ENDDO
CALL FORCES_long
```

$$
\begin{aligned}
&DO\ i = 1, Natoms \\
&VX(i) = VX(i) + 0.5*dt\_long*FX\_long(i) \\
&VY(i) = VY(i) + 0.5*dt\_long*FY\_long(i) \\
&VZ(i) = VZ(i) + 0.5*dt\_long*FZ\_long(i) \\
&ENDDO
\end{aligned} \tag{B1}
$$

In the above, the first loop uses the long range forces from the previous step to obtain the initial conditions on the velocities for the current step. The middle loop runs over the number of inner time steps and computes the reference system positions and velocities from the short range forces. The final loop corrects the velocities from the current values of the long range force. The routines *FORCES_short* and *FORCES_long* are assumed to update the short and long range components of the force, respectively, $dt\_short = dt\_long/FLOAT(Ninner)$, and $dt2\_short = (dt\_short)^2$.

[1] M. E. Tuckerman, G. J. Martyna, and B. J. Berne, J. Chem. Phys. **93**, 1287 (1990).
[2] M. E. Tuckerman, B. J. Berne, and A. Rossi, J. Chem. Phys. **94**, 1465 (1990).
[3] M. E. Tuckerman and B. J. Berne, J. Chem. Phys. **94**, 6811 (1991).
[4] S. Duane, A. D. Kennedy, B. J. Pendleton, and D. Roweth, Phys. Lett. B **195**, 216 (1987).
[5] M. Creutz and A. Goksch, Phys. Rev. Lett. **63**, 9 (1989).
[6] H. De Raedt and B. De Raedt, Phys. Rev. A **28**, 3575 (1983).
[7] M. Takahashi and M. Imada, J. Phys. Soc. Jpn. **53**, 3765 (1984).
[8] C. W. Gear, *Numerical Initial Value Problems in Ordinary Differential Equations* (Prentice-Hall, Englewood Cliffs, 1971).
[9] H. F. Trotter, Proc. Am. Math Soc. **10**, 545 (1959).
[10] W. C. Swope, H. C. Andersen, P. H. Berens, and K. R. Wilson, J. Chem. Phys. **76**, 637 (1982).
[11] J. C. Sexton and D. H. Weingarten, Nucl. Phys. B (in press); Nucl. Phys. B Proc. Suppl. **26**, 613 (1992).
[12] M. E. Tuckerman and B. J. Berne, J. Chem. Phys. **95**, 8362 (1991).
[13] M. P. Allen and D. J. Tildesley, *Computer Simulation of Liquids* (Oxford University, Oxford 1989).
[14] S. Nosé, Mol. Phys. **52**, 255 (1984).
[15] S. Nosé, J. Chem. Phys. **81**, 511 (1984).
[16] W. G. Hoover, Phys. Rev. A **31**, 1695 (1985).
[17] D. J. Evans and G. P. Morriss, *Statistical Mechanics of Nonequilibrium Liquids* (Academic, San Diego, 1990).
[18] M. E. Tuckerman and B. J. Berne, J. Chem. Phys. **95**, 4389 (1991).